THE JOURNAL OF BIOLOGICAL CHEMISTRY VOL. 285, NO. 23, pp. 17488–17497, June 4, 2010

Direct Measurements of the Outer Membrane Stage of Ferric Enterobactin Transport

POSTUPTAKE BINDING[*][S]

Received for publication, January 4, 2010, and in revised form, February 23, 2010 Published, JBC Papers in Press, March 24, 2010, DOI 10.1074/jbc.M109.100206

Salete M. Newton, Vy Trinh, Hualiang Pi, and Phillip E. Klebba[1]

From the Department of Chemistry and Biochemistry, University of Oklahoma, Norman, Oklahoma 73019

When Gram-negative bacteria acquire iron, the metal crosses both the outer membrane (OM) and the inner membrane, but existing radioisotopic uptake assays only measure its passage through the latter bilayer, as the accumulation of the radionuclide in the cytoplasm. We devised a methodology that exclusively observes OM transport and used it to study the uptake of ferric enterobactin (FeEnt) by *Escherichia coli* FepA. This technique, called postuptake binding, revealed previously unknown aspects of TonB-dependent transport reactions. The experiments showed, for the first time, that despite the discrepancy in cell envelope concentrations of FepA and TonB (~35:1), all FepA proteins were active and equivalent in FeEnt uptake, with a maximum turnover number of ~5/min. FepA-mediated transport of FeEnt progressed through three distinct phases with successively decreasing rates, and from its temperature dependence, the activation energy of the OM stage was 33–35 kcal/mol. The accumulation of FeEnt in the periplasm required the binding protein and inner membrane permease components of its overall transport system; postuptake binding assays on strains devoid of FepB, FepD, or FepG did not show uptake of FeEnt through the OM. However, fluorescence labeling data implied that FepA was active in the Δ*fepB* strain, suggesting that FeEnt entered the periplasm but then leaked out. Further experiments confirmed this futile cycle; cells without FepB transported FeEnt across the OM, but it immediately escaped through TolC.

Microbes overcome the paucity of environmental iron (1) by the elaboration of siderophores (1, 2), whose high affinity for Fe^{3+} extracts it from both inorganic polymers and mammalian proteins (3–6). Gram-negative bacteria transport ferric siderophores through outer membrane (OM)[2] receptor proteins, and the uptake of ferric enterobactin (FeEnt) (7) by the *Escherichia coli* OM protein FepA (8, 9) is prototypical of bacterial high affinity (subnanomolar) (10) metal acquisition systems. Siderophore receptors concentrate iron against a gradient, so their uptake reactions require energy. Another cell envelope protein, TonB (11, 12), performs an essential but still obscure role in metal transport. TonB action may equate with energy transduction, but this assumed synonymity (13–17) awaits a definitive demonstration and a mechanism. Completion of the OM stage releases FeEnt into the periplasm, where it associates with FepB (18, 19) and subsequently transfers to the FepCDGFes inner membrane (IM) complex (20, 21) that transports the iron chelate into the cytoplasm, hydrolyzes the organic ligand, and reduces the metal.

TonB may survey the periplasmic surface of the OM (22, 23) until it encounters and recruits a ligand-bound transporter (24, 25), thereby initiating the events that lead to metal internalization. However, the concentration of FepA in the OM is much greater than that of TonB in the periplasm (10, 26), and consideration of all *E. coli* TonB-dependent paralogs (*i.e.* FepA, Cir, FecA, Fiu, FhuA, FhuE, and BtuB) maximally expressed in iron-deficient conditions establishes an ~100-fold discrepancy between their total concentration and that of TonB (22). This disproportionality implies the existence of two populations of TonB-dependent proteins in the OM: active transporters associated with TonB and inactive transporters unassociated with it. It is unknown whether the sluggish overall rate of FeEnt uptake (k_{cat} ~5 min^{-1}) (23, 27, 28) results from the fact that at any instant only a fraction of FepA proteins associate with TonB or results from an intrinsically slow transport mechanism. We addressed this and other questions with a methodology that observes the internalization of FeEnt by FepA. We applied this assay to wild-type cells and strains lacking TonB, FepB, FepD, FepG, and TolC and made measurements of FeEnt uptake kinetics alone and during simultaneous transport of ferrichrome (Fc). This approach revealed that all of the FepA proteins in the OM equivalently participate in FeEnt uptake, that accumulation of FeEnt in the periplasm requires FepB and is modulated by TolC, that simultaneous transport of Fc has only small effects on FeEnt uptake but concomitant FeEnt transport causes a 50% drop in the rate of Fc uptake, and that the activation energy of FepA-mediated FeEnt transport is 33–35 kcal/mol.

EXPERIMENTAL PROCEDURES

Bacterial Strains, Plasmids, and Culture Conditions—Bacteria were grown at 37 °C with shaking to stationary phase in Luria-Bertani (LB) broth (29) containing streptomycin (100 μg/ml) and, when appropriate, chloramphenicol (10 μg/ml).

* This work was supported, in whole or in part, by National Institutes of Health Grant GM53836. This work was also supported by National Science Foundation Grant MCB0417694 (to P. E. K. and S. M. N.).

[S] The on-line version of this article (available at http://www.jbc.org) contains supplemental Figs. S1–S3.

[1] To whom correspondence should be addressed: Dept. of Chemistry and Biochemistry, University of Oklahoma, Norman, OK 73019. Tel.: 405-325-4969; E-mail: peklebba@ou.edu.

[2] The abbreviations used are: OM, outer membrane; IM, inner membrane; FeEnt, ferric enterobactin; Fc, ferrichrome; mAb, monoclonal antibody; MOPS, 3-(*N*-morpholino)propanesulfonic acid; FM, fluorescein 5-maleimide; CCCP, carbonyl cyanide *m*-chlorophenyl hydrazone; PUB, postuptake binding.

For binding and transport experiments, we subcultured strains at 1% from stationary phase LB cultures into iron-free MOPS minimal medium (30) with vigorous aeration at 37 °C for 5.5 h to an approximate $A_{600\ nm}$ of 0.8–0.9, which derepressed the Fur-regulated ferric siderophore transport systems. The experiments compared BN1071 (*F*−, *entA*, *pro*, *trp*, *B1*) (31), which contains a wild-type FeEnt uptake system, with its site-directed deletion derivatives OKN1 (Δ*tonB*) (32), OKN3 (Δ*fepA*) (32), OKN13 (Δ*tonB*, Δ*fepA*) (32), OKN4 (Δ*fepB*), OKN6 (Δ*fepC*), OKN11 (Δ*fepD*), OKN12 (Δ*fepG*), OKN34 (Δ*fepA*, Δ*fepB*), and OKN422 (Δ*fepB*, Δ*tolC*). We constructed the latter six strains by allelic replacement, creating precise, complete, in-frame deletions by transformation with linear PCR-generated DNA fragments (33), and verified the mutations by DNA sequence analysis of chromosomal PCR products. For some experiments, we introduced pFepAG54C or pFepAS271C (32) in OKN34 by electroporation.

Siderophores—We purified enterobactin (28) and apoferrichrome (27) from cultures of *E. coli* and *Ustilago sphaerogena*, respectively, and formed their iron complexes with ^{56}Fe or ^{59}Fe. We purified FeEnt and Fc by chromatography over Sephadex LH20 (Amersham Biosciences) (34) or DE52 (Whatman) (35), respectively. Both ^{56}Fe- and ^{59}Fe-labeled enterobactin were either prepared fresh or repurified for each experiment.

Postuptake Binding (PUB) Measurements of OM Transport—The passage of a single molecule of FeEnt through FepA occurs in 10–15 s (10, 23, 27, 28). If bacterial cells are saturated with ^{56}FeEnt at 0 °C (which allows its binding to FepA but not transport) and rapidly shifted to 37 °C for 1 min (which allows transport), then the FepA proteins that internalize the metal complex will become vacant and available for binding of ^{59}FeEnt. Because each FepA protein adsorbs a single molecule of FeEnt (8), the extent of subsequent ^{59}FeEnt binding reveals the number of receptors that were vacated because they successfully transported ^{56}FeEnt. Hence, PUB assays directly determine the quantity and fraction of active FepA proteins during the incubation at 37 °C, by afterward measuring their binding of ^{59}FeEnt (supplemental Fig. S1).

We performed this technique, which exclusively monitors OM transport, as follows. (i) We deposited 1 ml of freshly grown, late exponential phase MOPS cultures (~10^8 cells) into microcentrifuge tubes, chilled them on ice for 20 min, and added ^{56}FeEnt to 100 nM. After pelleting the bacteria by centrifugation at 4 °C for 1 min, we removed excess siderophore by carefully aspirating the supernatant and resuspended the cells in 100 μl of ice-cold MOPS medium. (ii) We allowed uptake of the bound ^{56}FeEnt by adding 900 μl of MOPS medium at 42 °C (instantaneously warming the cells to 37 °C) and incubating them 1 min in a 37 °C water bath. (iii) We chilled the cells on ice, pelleted and resuspended them in 1 ml of MOPS medium at 0 °C, diluted 100-μl aliquots into 10 ml of ice-cold MOPS medium containing varying concentrations of ^{59}FeEnt, collected the bacteria on nitrocellulose filters, and counted the filters to determine the extent of ^{59}FeEnt binding (10). This approach required two control experiments: (i) normal binding assays to measure ^{59}FeEnt adsorption at 0 °C to cells that were not previously exposed to ^{56}FeEnt (which measured the total FeEnt binding capacity); (ii) blocked binding assays that measured ^{59}FeEnt adsorption at 0 °C to cells previously saturated with ^{56}FeEnt at 0 °C but *not* subjected to the 37 °C transport phase (*i.e.* they were pelleted by centrifugation and resuspended in 1 ml of ice-cold MOPS medium; 100-μl aliquots were diluted into ice-cold MOPS containing ^{59}FeEnt and then filtered and counted). This assay measured the ^{56}FeEnt that dissociated from the bacteria into the buffer. In each case, the reported data were the average of three separate experiments, and in each individual experiment, the samples were assayed in triplicate.

Radioisotopic Iron Uptake Assays—We also measured ^{59}FeEnt and ^{59}Fc uptake by conventional radiochemical assays (10).

Initial Rate of FeEnt Uptake—For PUB measurements of the initial FeEnt OM transport rate, 1 ml of MOPS-grown BN1071 culture was chilled on ice, saturated with 100 nM ^{56}FeEnt, pelleted by centrifugation, resuspended in 100 μl of ice-cold MOPS medium, and mixed with 900 μl of MOPS medium at 42 °C, instantaneously warming the cells to 37 °C. 100-μl aliquots were removed at sequential 10-s intervals and diluted 250-fold into ice-cold MOPS medium. After 5 min on ice, ^{59}FeEnt was added to 25 nM and incubated for 1 min, the cells were collected on filters and washed with 0.9% LiCl, and filters were counted to determine the extent of ^{59}FeEnt binding.

Accumulation of FeEnt—^{59}FeEnt was added to 10 μM in a 3-ml aliquot of BN1071 culture in late exponential phase (5×10^8 cells/ml) at 37 °C. At the noted cell concentration and known V_{max} (150–200 pmol/10^9 cells/min; see below and Ref. 23), the ferric siderophore was sufficient to remain in excess for over 2 h. The culture was incubated at 37 °C with shaking, and 100-μl aliquots of cell suspension were removed at sequential time points over 90 min, filtered, washed, and counted to determine the extent of iron accumulation.

For determination of FeEnt retention by cells, ^{59}FeEnt was added to 0.5 μM in a 5-ml aliquot of BN1071 culture in late exponential phase (5×10^8 cells/ml) at 37 °C. Samples were withdrawn, filtered, washed, and counted at intervals for 40 min to determine the amount of ferric siderophore accumulated by the bacteria. Next, excess ^{56}FeEnt (10 μM final concentration) was added to the remaining culture, and aliquots were withdrawn, filtered, washed, and counted to determine the amount of the radionuclide retained by the cells during the subsequent uptake of non-radiolabeled FeEnt.

Transport in the Presence of Multiple Siderophores—For PUB determinations of FeEnt transport in the presence of Fc, cells were grown, chilled, and mixed with saturating amounts (100 nM) of both ferric siderophores; the excess was removed by centrifugation; and the cells were resuspended in 100 μl of MOPS medium containing 100 nM Fc. 900 μl of MOPS medium at 42 °C was added, and the cells were transferred to a 37 °C water bath and incubated for 1 min to allow ferric siderophore uptake. The extent of ^{56}FeEnt uptake was determined by the subsequent binding of ^{59}FeEnt, as discussed above.

Fluorescence Labeling—We spectroscopically measured the transport of FeEnt through FepA by fluoresceinating OKN3/pFepAS271C (32, 36) and incubating 5×10^6 bacterial cells with FeEnt in an SLM-AMINCO 8000 fluorometer (Rochester, NY) upgraded to 8100 functionality (36). With excitation and emission wavelengths at 490 and 518 nm, respectively, we observed the quenching caused by FeEnt binding to

FepAS271C-FM and its ultimate reversion by FeEnt transport (36).

Electrophoresis and Western Immunoblots—For SDS-PAGE (37), samples were prepared in sample buffer with 3% β-mercaptoethanol, boiled for 5 min, and electrophoresed at 30 mA. For Western immunoblots, the proteins were transferred to nitrocelullose paper, which was blocked for 10 min with TBS (50 mM Tris chloride, pH 7.5, 0.9% NaCl) plus 1% gelatin, and incubated with appropriate mouse or rabbit primary antisera in the same buffer. For visualization of FepA, we used mouse monoclonal antibody (mAb) 45 (38); for FepB we used mouse mAbs 2, 4, 23, and 28 (19); and for TonB, we used rabbit polyclonal antibodies (23). After incubation and washing 5 times with tap water, the filter was incubated with alkaline phosphatase-conjugated goat anti-mouse or goat anti-rabbit IgG or ^{125}I-protein A. The paper was washed five times with tap water, and the immunoblot was developed by the addition of nitro blue tetrazolium and bromochloroindoyl phosphate or visualized on a StormScanner (Amersham Biosciences), respectively.

FepA-FepB Co-immunoprecipitation—To test the possibility that FepB interacts with FepA at the periplasmic interface of the OM, we immunoprecipitated FepA with an IgG2b monoclonal antibody in the presence of FepB and FeEnt and analyzed the precipitate by SDS-PAGE. Although the binding of mAb 45, which recognizes an epitope in FepA L4, near residue 329 (39) inhibits FeEnt adsorption and uptake (38), flow cytometric analyses showed that the binding of FeEnt to FepA does not block the adsorption of mAb 45 (data not shown). Before the addition to the reaction mixture, the component solutions of FepA, mAb 45, and FepB were centrifuged at 18,000 × *g* for 5 min to remove precipitates. After preliminary experiments to determine the optimum order and concentrations of reagents for formation of an immune complex, we incubated FepA (4.5 μg) with or without FeEnt (10 nM) for a few s, before the addition of FepB (15.4 μg) and anti-FepA mAb 45 (30 μg), in a final volume of 0.5 ml of TBS. We allowed the suspension to sit overnight 4 °C, and in the morning we added 50 μl of protein A-agarose (Pierce immobilized protein A plus; contains protein A at 3 mg/ml resin) and allowed the mixture to incubate for an additional 2 h at room temperature. Immune complexes were pelleted by centrifugation at 5000 × *g* for 5 min, solubilized in sample buffer, and analyzed by SDS-PAGE.

Determination of the Activation Energy of FeEnt Transport through FepA—FeEnt binding to FepAS271C-FM quenches its fluorescence emissions (40), but as live bacteria deplete the ferric siderophore from solution by transport, the fluorescence rebounds. From such spectroscopic measurements (36) we determined the rate constants for the FeEnt OM transport reaction in two ways. In the first case (time to depletion threshold method), we initially saturated the cells with 10 nM FeEnt and measured the elapsed time for them to deplete it from solution.

$$\text{FepA} + \text{FeEnt}_{\text{out}} \underset{k_{-1}}{\overset{k_1}{\rightleftharpoons}} \text{FepA-FeEnt} \xrightarrow{k_2} \text{FepA} + \text{FeEnt}_{\text{in}}$$

REACTION 1

$$v = k_2[\text{FepA-FeEnt}] \quad \text{(Eq. 1)}$$

FeEnt was in excess during this period, so $v = V_{max}$ and [FepA-FeEnt] = [FepA]. Therefore, the following was true.

$$V_{max} = k_2[\text{FepA}] \quad \text{(Eq. 2)}$$

To determine V_{max} by this method we measured the time (s) from the point of the FeEnt addition until F/F_o inflected upward (to an arbitrary value of 0.4), at which point ~20 pmol of FeEnt were transported by the cells. From V_{max} at each temperature and the concentration of FepA (5 nM), we found k_2.

In the second case (depletion rate method), after the bacteria reached the depletion threshold, as transport continued and [FeEnt] further decreased, FepAS217C-FM underwent a linear unquenching that reverted fluorescence to its original level. At the midpoint of the unquenching curve, FepA was half-saturated with FeEnt, so the following was true.

$$v = V_{max}/2 = k_2[\text{FepA}]/2 \quad \text{(Eq. 3)}$$

In this case, the slope of the reversion curve was proportional to v, and from the concentration of FepA (5 nM), we found k_2. We plotted log (k_2) against $1/T$ and obtained the activation energy (E_a) from the Arrhenius equation, $k = Ae^{-E_a/RT}$ (41). These calculations were approximations, but whether k_2 derived from the elapsed time to the depletion threshold or from the depletion rates at half-saturation, it proportionally reflected the temperature dependence of FeEnt transport.

RESULTS

Proportion of FepA Proteins That Transport FeEnt—The discrepant cell envelope concentrations of FepA and TonB intimate that at any given time only a fraction of FepA proteins actively transport FeEnt, which potentially explains the receptor's low turnover number (about 3–5 min^{-1}) (10, 23, 28). We employed PUB experiments to clarify this point. When the population of FepA proteins is saturated with ^{56}FeEnt, if only a fraction of the transporters participates in its uptake, then only that fraction will become vacant and capable of binding ^{59}FeEnt. If, on the other hand, all of the FepA proteins with bound ^{56}FeEnt transport it, then they will all be free to bind ^{59}FeEnt. PUB experiments measure the number of FepA proteins that transport FeEnt through the OM, without dependence on subsequent uptake of the ligand through the IM into the cytoplasm.

For these studies, it was necessary to measure the dissociation of bound FeEnt from FepA in live bacteria. Transfer of cells that are saturated with FeEnt into fresh medium results in re-equilibration of the receptor-ligand interaction, as dictated by their concentrations and the affinity of the association. In practice, the cells release some of the bound ligand, and we measured this quantity for strain BN1071, which expresses wild type FeEnt transport components from single copy chromosomal genes (20, 31). Cells of BN1071 were chilled on ice and incubated with 100 nM ^{56}FeEnt at 0 °C, which saturated FepA proteins (K_D = 0.2 nM) (10, 39). The iced cells were incapable of actively transporting the ligand through the OM, and when cells with bound ^{56}FeEnt at 0 °C were collected by centrifugation and resuspended in ice-cold buffer, approximately one-third of their FepA proteins became free to adsorb ^{59}FeEnt; *i.e.*

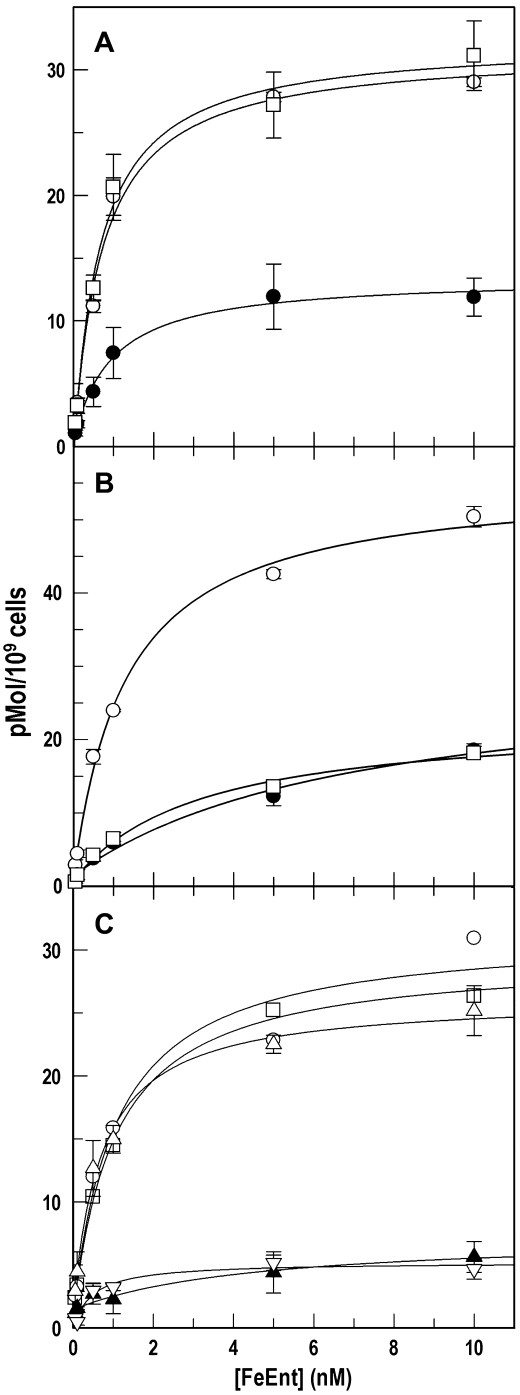

FIGURE 1. **PUB determinations of FeEnt uptake by *tonB*$^+$ and Δ*tonB E. coli* strains in the absence and presence of CCCP.** Bacteria were cultured in MOPS medium and subjected to PUB assays as described under "Experimental Procedures." In *A* (BN1071: *tonB*$^+$) and *B* (OKN1: Δ*tonB*), we compared ^{59}FeEnt binding capacity in three conditions: normal binding (○), blocked binding (●), and PUB (□). In *C*, BN1071 was assayed for normal binding (○) and PUB (□) as in *A*, and the same cells were assayed after a 30-min exposure to 0.5 mM CCCP (normal binding (△), blocked binding (▲), and PUB (▽)). For clarity, S.E. (*error bar*) estimates in *C* are only shown for CCCP-treated samples. BN1071 transported the bound FeEnt, but neither Δ*tonB* cells nor energy-depleted cells internalized the ferric siderophore through FepA.

^{56}FeEnt dissociated from a third of the FepA proteins during the manipulations, and two-thirds of the receptor proteins retained the bound ligand and therefore did not adsorb ^{59}FeEnt (blocked binding; Fig. 1). We observed little variation in the

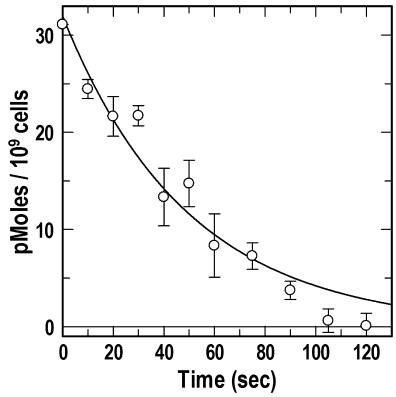

FIGURE 2. **Initial kinetics of FeEnt OM transport from PUB determinations.** BN1071 was chilled on ice, saturated with ^{56}FeEnt in 100 μl of ice-cold MOPS, and then diluted to 1 ml in MOPS medium at 42 °C, instantaneously warming them to 37 °C. Aliquots were removed at sequential 10-s intervals and diluted 250-fold into ice-cold MOPS, and after 5 min, ^{59}FeEnt was added to 25 nM, and the cells were filtered, washed, and counted to determine the extent of ^{59}FeEnt binding. The results (○) are plotted as the depletion of bound ^{56}FeEnt from the cell surface by uptake. *Error bars*, S.E.

^{56}FeEnt dissociation/retention level for any individual strain. Against this background, we performed the same procedures, except that after saturation with ^{56}FeEnt at 0 °C, centrifugation, and resuspension in cold buffer, we jumped the temperature to 37 °C for 1 min to allow transport of bound ligand before recooling to 0 °C and assay with ^{59}FeEnt. In BN1071, all FepA proteins with bound ^{56}FeEnt were functional during the incubation at 37 °C, in that they internalized it and then adsorbed ^{59}FeEnt to full capacity (Fig. 1). The difference between the blocked binding and the PUB values revealed the extent of FeEnt OM transport. Non-functional FepA proteins (in the TonB-deficient strain OKN1 (Δ*tonB*) or in CCCP-treated BN1071) did not transport ^{56}FeEnt after the temperature jump and hence did not bind additional ^{59}FeEnt.

Initial Rate of FeEnt Uptake by FepA—Standard radioisotopic iron uptake assays quantify the accumulation of the metal across the IM into the cytoplasm, but because the OM stage is rate-limiting in the overall process, such determinations reflect OM transport rates. We sought an independent measurement of the low FepA and FhuA turnover numbers and employed PUB assays to directly monitor the OM transport reaction. Uptake began immediately and continued until all FepA proteins were vacated (about 90 s; Fig. 2). The transport reaction was a first order process with $k = 1.2$ min^{-1}, which was consistent with, although slightly slower (3-fold) than, the previously measured rate. However, whereas previous determinations evaluated bacteria during exponential growth at 37 °C, in PUB assays, the cells were initially chilled on ice, exposed to FeEnt, and then rewarmed to physiological temperature. We suspected that the 3-fold slower rate derived from this difference in protocols and performed conventional ^{59}FeEnt uptake assays with cells chilled on ice prior to assay at 37 °C to test this supposition; V_{max} was 83 pmol/10^9 cells/min for the first 20 s (compared with 208 pmol/10^9 cells/min for exponentially growing cells at 37 °C (23)), and the rate approximately doubled to 172 pmol/10^9 cells/min for the succeeding 40 s (data not shown). These data translated into turnover numbers of 1.2/min for the first 20 s, 2.6/min for the next 40 s, and a mean value

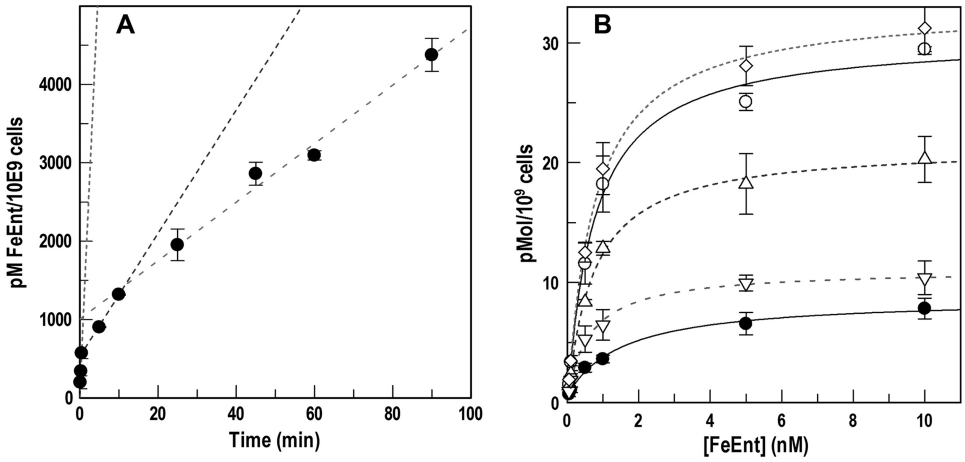

FIGURE 3. **Temporal dependence of FeEnt uptake.** *A*, conventional assays of ^{59}FeEnt accumulation. BN1071 was grown in MOPS medium to midlog, excess ^{59}FeEnt (10 μM) was added, and aliquots were removed and counted over a 90-min period (●). The accumulation time course was triphasic (fitted curves: ····, - - - -, – – – –). *B*, PUB determinations of FeEnt transport rates. Bacteria were grown as in *A*, and ^{56}FeEnt was added to 10 μM at $t = 0$. Before its addition and at 5 and 20 min afterward, aliquots of cells were collected by centrifugation, resuspended in fresh MOPS medium for 1 min at 37 °C, and assayed for PUB of ^{59}FeEnt over a range of concentrations. We measured normal binding (○), blocked binding (●), and PUB at $t = 0$ (◇), 5 (△), and 25 min (▽). The experiment found three different rates of FeEnt uptake at $t = 0$ (····), 5 (- - - -), and 20 min (– – – –). *Error bars*, S.E.

of 2 for the 1-min assay period. Thus, chilling the cells retarded the uptake of FeEnt during the first min of rewarming, explaining the lower rate found by the PUB tests.

Kinetics of ^{59}FeEnt Accumulation—We exposed BN1071 to ^{59}FeEnt at 10 μM, a sufficiently high concentration to avoid depletion during transport at V_{max} for ~2 h, and measured the time course of FeEnt accumulation by conventional radioisotopic measurements over a 90-min duration. These data (Fig. 3) showed three uptake stages by the chromosomally encoded FeEnt transport system: an initial phase at maximum rate during the first 30 s (V_{max} = 150 pmol/min/10^9 cells), which was consistent with previous measurements (10, 28); a secondary phase in the ensuing 10 min with an intermediate rate (V_{max} = 78 pmol/min/10^9 cells); and a final, apparently steady state phase of lowest rate (V_{max} = 37 pmol/min/10^9 cells) that persisted to the end of the 90-min period. To further understand the triphasic time course, we made PUB assays of FepA activity during the three stages, at 15 s and at 5 and 25 min. The results confirmed the existence of three different uptake rates at the three time points (Fig. 3). Alterations in the amount of FepA in the OM did not explain the stepwise 2-fold and >5-fold decrease in rate that occurred by $t = 20$ min, because quantitative immunoblot determinations of FepA concentration (10) showed no significant variation at the three sequential time points (data not shown). These results indicated that a decrease in the transport rate through FepA caused the drop in overall FeEnt accumulation into the cytoplasm (19), suggesting that other cell envelope or intracellular processes regulate the OM transport activity of FepA. The FeEnt uptake rate was inversely proportional to the amount accumulated by the cells and reached a steady state within about 10 min.

FepA-mediated FeEnt Uptake in Bacteria Devoid of FepB, FepD, or FepG—We genetically engineered (33) in-frame deletions of the *fepB*, *fepD*, and *fepG* loci in BN1071 and verified the expected structures of the deletions by DNA sequence analysis. The mutant strains were inactive in siderophore nutrition tests with FeEnt and unable to accumulate any ^{59}FeEnt in conventional uptake assays (data not shown). We also employed PUB assays to measure FepA transport, and none of the four strains measurably internalized bound FeEnt through the OM (Fig. 4). Although we anticipated their inability to accumulate FeEnt into the cytoplasm, we did not expect their complete lack of FepA-mediated OM transport.

The defects in FeEnt uptake as a result of Δ*fepB* raised the possibility of an interaction between the binding protein and FepA during the OM transport reaction. To test this idea, we immunoprecipitated FepA with an IgG2b antibody that recognizes an epitope in surface loop 4 (anti-FepA mAb 45) (38, 39) in the presence or absence of FepB and FeEnt (10 nM). The immunochemical reaction precipitated FepA from solution, but FepB did not co-precipitate, whether or not FeEnt was present. These data (supplemental Fig. S2) argued against the notion that FepB actively mediates the passage of FeEnt into the periplasm by a direct interaction with FepA. We repeated the experiment but in this case precipitated FepA in OM fragments (42) by ultracentrifugation, in the presence of FepB and FeEnt, with the same results (supplemental Fig. S3); FepB did not detectably bind to FepA under any conditions.

Specific sites within FepA are chemically modifiable during binding and transport of FeEnt (32, 43), and chemical modification of the substitution G54C occurs during active FeEnt uptake. Located in the N-domain of FepA, G54C is susceptible to fluoresceination during FeEnt transport (32) but not labeled in *tonB* or energy-poisoned cells. We introduced pFepAG54C into OKN3 (Δ*fepA*), OKN34 (Δ*fepA*, Δ*fepB*), and OKN13 (Δ*tonB*, Δ*fepA*) host strains and compared their FM labeling patterns (Fig. 5). G54C was modified by FM when FeEnt was present, regardless of whether the host strain was *fepB*$^+$ or Δ*fepB*, but it was not modified in the Δ*tonB* host. These data implied that FepA-mediated FeEnt transport activity did occur in the absence of FepB.

Because the PUB assays and spectroscopic experiments gave different results, we performed additional studies on the retention of ^{59}FeEnt by wild-type (BN1071), Δ*tonB* (OKN1), and Δ*fepB* (OKN4) bacteria, comparable with those conducted by Bradbeer (44) with BtuB. BN1071 rapidly acquired ^{59}FeEnt from solution (Fig. 5*B*) and retained it even if subsequently exposed to excess ^{56}FeEnt. On the other hand, OKN4 absorbed little ^{59}FeEnt, and excess ^{56}FeEnt released most of the radiolabeled siderophore from the strain (Fig. 5, *B* and *C*). These data indicated that without periplasmic binding, FeEnt exchanged across the OM, as postulated for vitamin B$_{12}$ (44). Thus, in PUB assays of OKN4, FepA internalized FeEnt, but without FepB in the periplasm to bind it, the iron complex leaked out and

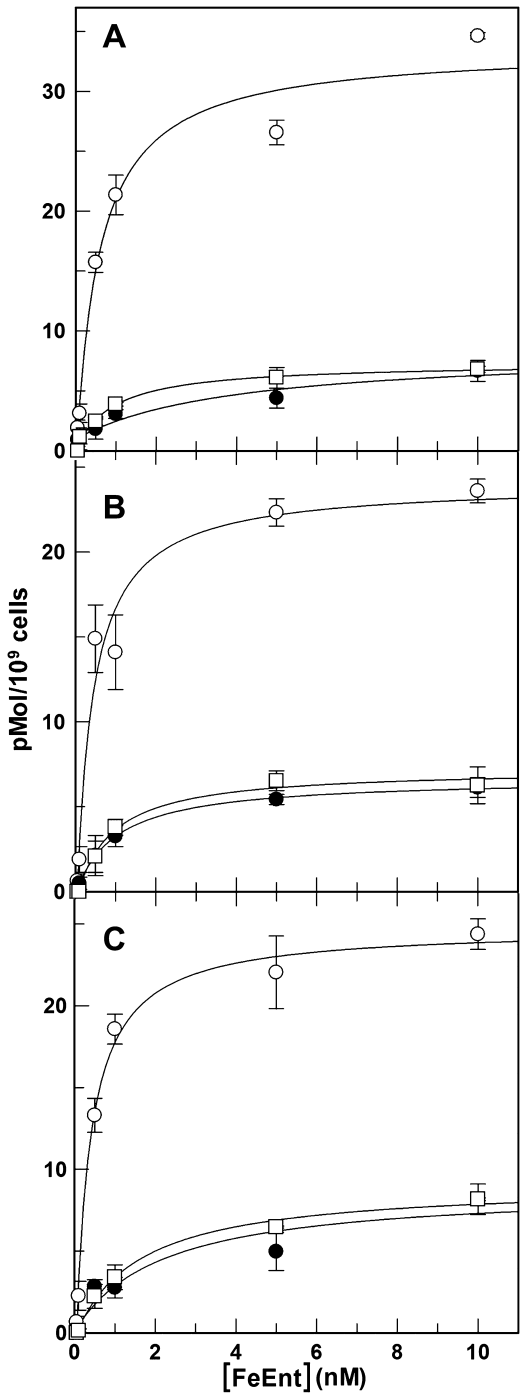

FIGURE 4. **PUB measurements of strains lacking FepB, FepD, or FepG.** MOPS-grown OKN4 (Δ*fepB*; *A*), OKN11 (Δ*fepD*; *B*), and OKN12 (Δ*fepG*; *C*) were subjected to PUB assays to assess their ability to transport FeEnt through FepA in the OM. The three strains were tested by normal ^{59}FeEnt binding procedures (○), blocked binding conditions (●), and PUB (□) as in Fig. 1*A*. None of the three strains showed any accumulation of bound FeEnt. *Error bars*, S.E.

rebound to FepA, creating a futile cycle that prevented subsequent adsorption of ^{59}FeEnt.

Besides its involvement in antibiotic export, TolC was implicated in the export of newly synthesized enterobactin from *E. coli* (45). We generated a Δ*fepB* Δ*tolC* derivative (OKN422) and subjected it to the same experiment. Unlike OKN4, OKN422 acquired nearly as much ^{59}FeEnt as cells with an intact FeEnt uptake system, and it retained it when exposed to excess ^{56}FeEnt (Fig. 5*B*). Thus, the Δ*tolC* mutation prevented exchange of FeEnt across the OM. Again unlike OKN4, PUB assays of OKN422 revealed FepA-mediated uptake of FeEnt into the periplasm (Fig. 5*D*). These data confirmed that in the absence of FepB, FepA transported FeEnt across the OM, but without the binding protein to adsorb it, the metal complex escaped from the cells. The results also identified the protein responsible for FeEnt release through the OM: TolC.

Simultaneous TonB-dependent Uptake of Two Ferric Siderophores—TonB functions in the uptake of all ferric siderophores through the OM. The fact that it physically contacts the OM receptor proteins implies that simultaneous transport of different ferric siderophores will competitively inhibit their individual rates of ligand internalization. Using both conventional radioisotopic assays and PUB determinations, we studied the effect of concomitant ferrichrome uptake at V_{max} on the kinetics of FeEnt transport, and vice-versa. Saturating concentrations of Fc had little discernible effect on the uptake of ^{59}FeEnt in standard uptake assays (Fig. 6); K_m and V_{max} of the FeEnt acquisition reaction were unchanged relative to the same parameters in the absence of Fc. PUB measurements, on the other hand, showed a 20% decrease in the V_{max} of FeEnt uptake when Fc was present. When the situation was reversed, saturating FeEnt markedly reduced V_{max} of ^{59}Fc transport (by about 50%), which was apparent even in conventional radioisotopic uptake assays (Fig. 6).

Activation Energy of FeEnt Transport through the OM—From fluorescence spectroscopic observations of FeEnt uptake at different temperatures (36), we used the Arrhenius equation to calculate the activation energy of the OM stage of FeEnt transport. When bacteria expressing FepAS271C-FM were exposed to 10 nM FeEnt, binding of the ferric siderophore quenched fluorescence emissions, but as the cells transported the ligand, they depleted it from solution, ultimately reversing the quenching effect. We determined the temperature dependence of the uptake rate in two ways: from the time required to deplete FeEnt (10 nM) from solution (elapsed time to the depletion threshold) and from the steady-state uptake rate at half-saturation. In the former case, we monitored the time from the point of FeEnt addition (maximum quenching) until F/F_o inflected upward and reached a value of 0.4 (Fig. 7). In the latter case, we measured the rate at which fluorescence rebounded when transport depleted the externally supplied FeEnt; as the concentration of ferric siderophore decreased, FepAS271C-FM underwent a linear unquenching that reverted fluorescence to its original level (Fig. 7). Calculations by both methods resulted in a linear dependence of log k_2 *versus* $1/T$, and the two approaches corroborated each other; the depletion threshold analysis gave a slope of −17,997 K, and a calculated activation energy of 35.8 kcal/mol; the depletion rate analysis resulted in a slope of −16,670 K and a calculated activation energy of 32.7 kcal/mol.

DISCUSSION

The PUB experiments directly measured the transport activity of FepA, allowing us to study some unresolved aspects of a TonB-dependent uptake system. The energy dependence of

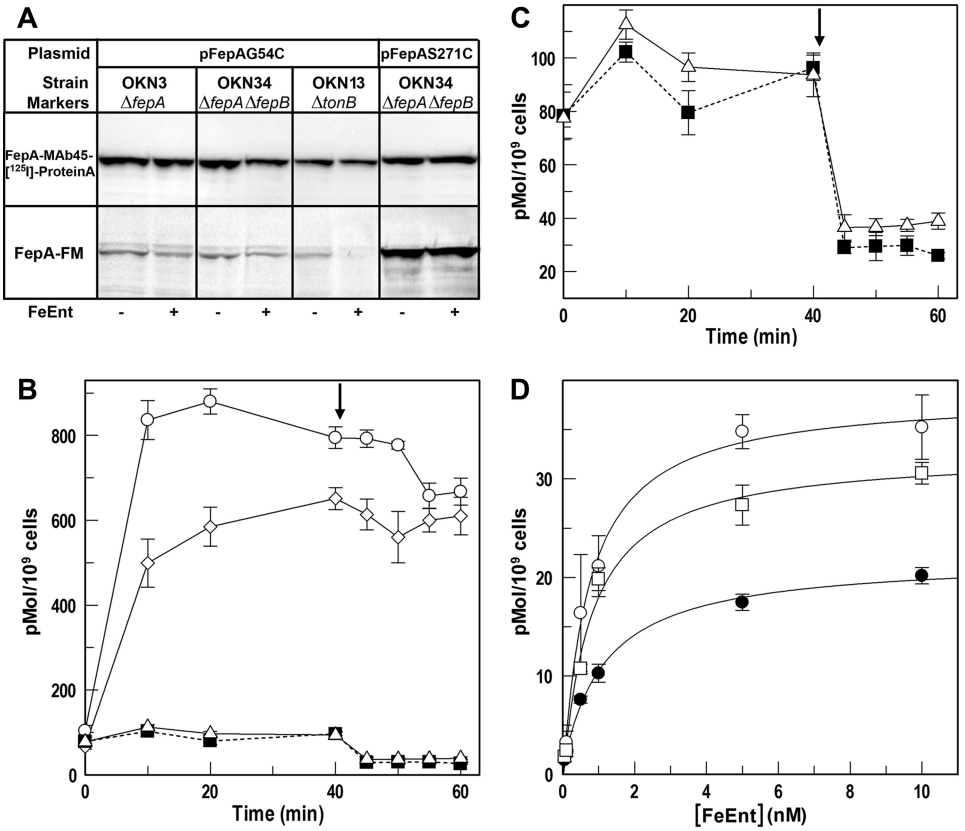

FIGURE 5. *A*, site-directed fluorescence labeling of OKN34/pFepAG54C during FeEnt uptake. To assess the functionality of FepA in the absence of FepB, we treated OKN3 (Δ*fepA*), OKN34 (Δ*fepA*, Δ*fepB*), and OKN13 (Δ*tonB*, Δ*fepA*), harboring pFepAG54C or pFepAS217C with 5 μM fluorescein maleimide during uptake of 10 μM FeEnt at 37 °C. Anti-FepA immunoblots (*top lanes*) showed that FepA was comparably expressed in all of the strains and conditions. Fluorescence scans of the same gels (*bottom lanes*) showed that in OKN3 and OKN34, the extrinsic fluorophore labeled FepAG54C, implying that the OM protein transported FeEnt (32). Conversely, in the Δ*tonB* strain OKN13, that binds FeEnt but does not transport it, we did not observe any modification of FepAG54C. Site FepAS271C, on the external surface of FepA, was comparably labeled in OKN34 whether or not FeEnt was present. *B* and *C*, retention of ^{59}FeEnt during subsequent exposure to ^{56}FeEnt. BN1071 (○), OKN1 (■), OKN4 (△), and OKN422 (Δ*fepB*, Δ*tolC*) (◇) were exposed to 0.5 μM ^{59}FeEnt for 40 min, and ^{56}FeEnt was added to 10 μM (*arrow*). Aliquots were collected at the indicated times, filtered, washed, and counted. *C* shows the drop in radioactivity of the Δ*tonB* and Δ*fepB* strains in greater detail. *D*, PUB measurements of bacteria lacking TolC and FepB. MOPS-grown OKN422 was subjected to PUB assays to assess its ability to transport FeEnt through FepA in the OM. The strain was tested by normal ^{59}FeEnt binding procedures (○), blocked binding conditions (●), and PUB (□) as in Fig. 1*A*. The deletion of TolC restored the ability to accumulate FeEnt in the periplasm, even in the absence of FepB. *Error bars*, S.E.

OM iron transport was one such consideration. Natural environmental amounts of ferric siderophores do not exceed micromolar levels, but typical cytoplasmic iron concentrations are in the millimolar range (46–48). Hence, the energy dependence of iron uptake by *E. coli* B/r (49) was not surprising because it was originally presumed relevant to the IM transport stage. Without explicit demonstrations, nevertheless, subsequent results suggested that OM metal transport also required energy. The facts that T1 and ϕ80 needed energy for irreversible adsorption to FhuA (TonA) (50) and that vitamin B_{12} uptake across the OM was inhibited by energy poisons (44, 51, 52), inferred that TonB-dependent transporters catalyzed active OM transport. However, general porins (OmpF, OmpC, PhoE, etc.) in the OM create $>10^5$ water-filled, 10-Å diameter channels per cell (53), eliminating the possibility of a trans-OM ion gradient as a driving force for metal uptake. This constraint led to the idea that TonB itself transduces energy to OM proteins, by membrane fusion (54) or intra-cell envelope protein-protein interactions (13, 14, 55–57) or by rotational motion (22, 23, 58–60). With some exceptions (32, 36), prior descriptions of ferric siderophore acquisition observed OM transport as the rate-limiting step in overall uptake through the cell envelope (10, 28, 51–53, 61–63), whose attributes were revealed by analysis of cytoplasmic iron accumulation. PUB determinations, on the other hand, observed internalization of the metal complex by FepA, ultimately emphatically demonstrating that both Δ*tonB* and proton motive force depletion prevent OM transport of FeEnt.

The amount of energy needed for the proton motive force- and TonB-dependent OM stage of iron uptake was unknown. Regarding FepA-FeEnt transport, Arrhenius calculations converged on an activation energy of 33–36 kcal/mol. It is a high value for a biochemical reaction, which translates into a Q_{10} value of 6–7 (64). Reactions with $Q_{10} > 2$ usually involve significant conformational changes, and the higher value for a TonB-dependent transporter presumptively reflects the need to rearrange its N-domain, or to expel it from the transmembrane channel, during ligand internalization. The noted bioenergetic quantity equates to hydrolysis of about 4 ATPs per molecule of FeEnt transported through FepA. Estimates of the amount of iron associated with bacteria grown in batch culture range from 0.1 to 0.25 mg/g dry weight (46–48), which translates into $0.6–1.6 \times 10^6$ atoms/cell, and an approximate intracellular concentration of 0.66–1.7 mM. If an individual cell acquires this quantity of external iron per cell division, then it will expend the equivalent of $2.4–6 \times 10^6$ ATPs to transport FeEnt *through the OM alone* during a division cycle. Additional energy expenditure, by direct ATP hydrolysis (the exact amount is currently undefined), promotes FeEnt transport through the FepCDG-Fes ABC transporter complex in the IM. Thus, substantial energy consumption occurs during iron acquisition, but it is still only a fraction of that required for other cellular process (*e.g.* ~0.1% of the energy expended for protein synthesis during a cell cycle).

PUB experiments additionally clarified the impact of stoichiometry on the relationship between OM metal transporters and TonB. The recruitment of TonB-box polypeptides of ligand-bound ferric siderophore receptors by the monomeric TonB

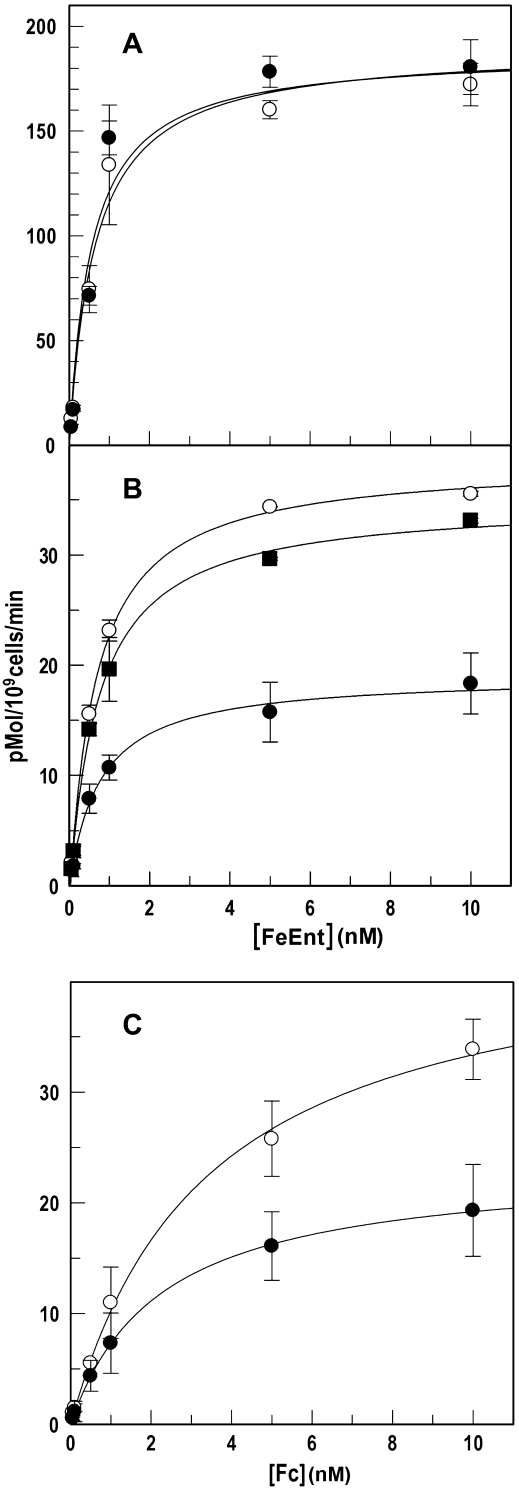

FIGURE 6. **Concomitant transport of FeEnt and Fc.** BN1071 was grown in MOPS medium. *A*, conventional measurements of ^{59}FeEnt uptake in the presence of Fc. The bacteria were assayed for ^{59}FeEnt uptake over a range of concentrations in the absence (○) and presence (●) of 100 μM Fc, which had no apparent effect by this protocol. *B*, PUB measurements of FeEnt uptake. The bacteria were tested for ^{59}FeEnt binding in normal (○) or blocked (●) conditions or in PUB assays in the presence of 100 μM Fc (■). *C*, conventional measurements of ^{59}Fc uptake in the presence of FeEnt. Cells were tested for ^{59}Fc uptake over a range of concentrations in the absence (○) and presence (●) of 100 μM FeEnt, which decreased V_{max} of the hydroxamate siderophore ~50%. *Error bars*, S.E.

C-terminus (24) probably initiates the OM transport process. Therefore, the relative abundances of OM transporters and TonB may influence metal uptake rates as a result of competition among ligand-bound receptors for the limited number of TonB proteins. Decreased OM uptake rates during simultaneous transport of FeEnt and Fc support this idea. The 50% inhibition of FhuA-mediated Fc transport by concomitant activity of FepA was consistent with the much higher abundance of the ferric catecholate transporter in the OM. ^{59}FeEnt capacity and quantitative immunoblots estimate the maximum concentration of chromosomally derived FepA as 35,000/cell in bacteria with derepressed iron acquisition systems (23). Measurements of TonB concentration show a maximum of 1000 copies/cell (26), indicating a 35-fold difference in the amounts of FepA and TonB. These calculations imply that at any instant, only about 3% of the OM-resident FepA may associate with TonB, which raises the question of what fraction of the FepA population actually transports FeEnt? If only this small percentage of total FepA proteins are active, then its V_{max} from traditional uptake assays (5–6/min) (23) underestimates an individual protein's transport rate as much as 30-fold. PUB experiments showed that when bacteria were shifted to 37 °C, the population of FeEnt-saturated FepA molecules exponentially decayed at a rate of 1.2/min and was depleted within 80 s. Hence, all FepA proteins with bound ligand transported it, implying that TonB identified and functionally interacted with all of them during that time. These data eliminate the possibility that only a fraction of the receptor population is functionally active. Therefore, within 80 s, each TonB protein located and facilitated transport of ~30 FepA proteins. It is conceivable that this identification/facilitation activity by TonB is the rate-limiting step of metal transport, potentially explaining the low overall turnover numbers of ferric siderophore transporters.

The protein framework underlying Gram-negative bacterial metal acquisition encompasses several layers of complexity in the trilaminar cell envelope: an OM receptor protein, the IM/OM-spanning TonB-ExbB-ExbD complex that may energize the OM stage, a periplasmic binding protein, an IM ABC transporter, and in some cases an N-terminal extension of the OM transporter that is tied to transcriptional regulation (65, 66). The PUB approach resolved the FeEnt OM transport process into three temporal phases: a rapid initial phase that persisted for about 30 s, a secondary stage that occurred from 0.5 to 10 min, and an ultimate, steady-state rate that continued indefinitely, from 10 to 90 min. These previously unobserved phases may reflect mechanistic connections to TonB-ExbBD, FepB, and FepCDG-Fes. The rate measurements begin with TonB presumably unassociated with (ligand-free) FepA or other metal transporters and neither FepB nor FepCDG-Fes occupied by FeEnt. In the second stage, at least TonB and FepB become saturated by their binding partners, and the binding protein transfers the ferric siderophore to the IM permease complex. In the final stage, all transport system proteins are saturated by FeEnt or FeEnt-bound proteins. The limited amounts of TonB (10, 26), FepB (19), and FepCDG-Fes in the cell envelope, relative to that of FepA, suggests that at steady state, a functional interaction among these proteins may

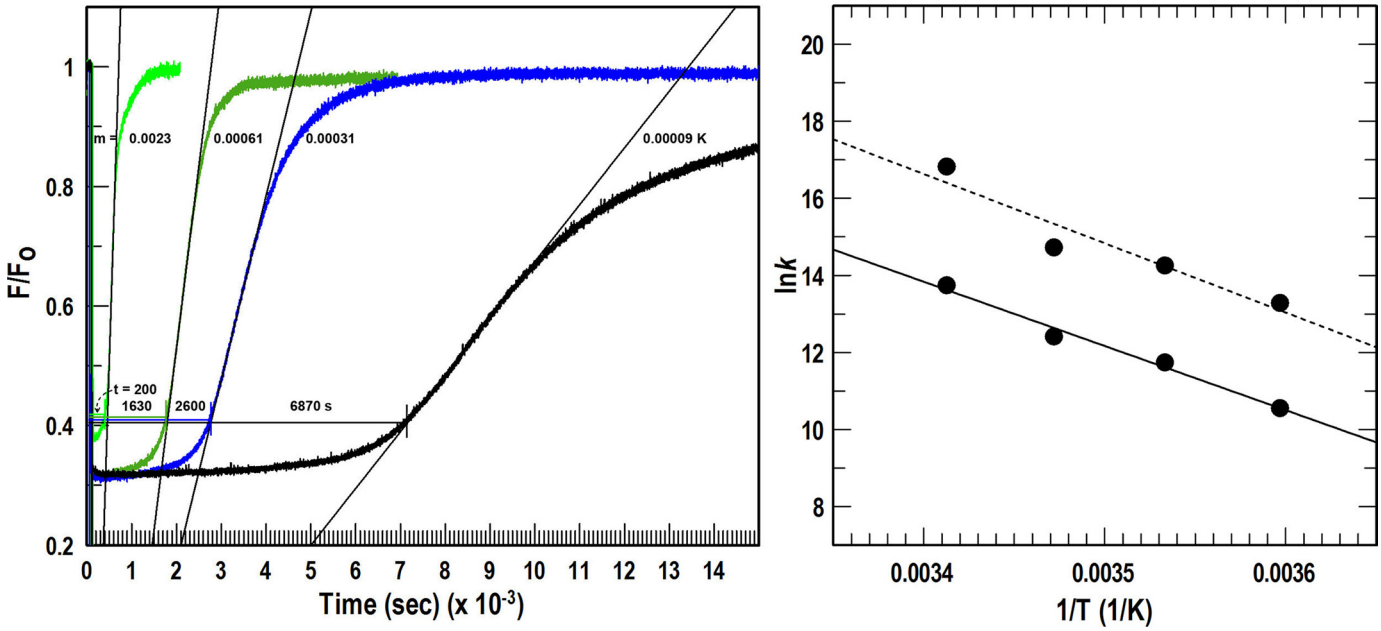

FIGURE 7. **Activation energy of the OM stage of FeEnt uptake.** *Left*, temperature dependence of quenching. We analyzed data from spectroscopic observations of FeEnt uptake (Fig. 3*c* of Ref. 36) to determine the activation energy of the OM transport reaction. The addition of 10 nM FeEnt (at $t = 0$) quenched the fluorescence of FepAS271C-FM, but the emissions reverted to initial levels when transport depleted the ferric siderophore from solution. We used the elapsed time at 20 °C (*green curve*), 15 °C (*dark green curve*), 10 °C (*blue curve*), and 5 °C (*black curve*) until the fluorescence tracing inflected upward (200, 1630, 2600, and 6870 s, respectively) and the rates of the fluorescence recovery at the different temperatures (slopes of the curves at half-saturation; $m = 0.0023$, 0.00061, 0.00031, and 0.00009 K, respectively) to calculate the relationship between temperature and uptake rate (k_2). *Right*, Arrhenius plots of log (rate) *versus* 1/*T*. We processed the data at the *left* according to $\ln(k) = \ln A - E_a/RT$, which when plotted (●) gave E_a values of 32.7 and 35.8 kcal/mol of FeEnt transported for the depletion rate (*dashed line*) and depletion threshold (*solid line*) methods, respectively.

become rate-limiting, but existing data do not yet identify this subreaction.

The absence of FeEnt uptake through FepA in strains lacking FepB, -D, or -G was unexpected and without obvious explanation, intimating that FepA was non-functional without a periplasmic binding protein or an active IM permease complex. Bacteria lacking these components were superficially equivalent to Δ*tonB* mutants: no stimulation by FeEnt in siderophore nutrition tests, no ^{59}FeEnt acquisition in standard uptake assays, and no measurable OM transport. Bradbeer (44) found that after [^{57}Co]vitamin B_{12} enters the OM through BtuB, without IM transport the periplasmic pool exchanges with vitamin B_{12} outside the cell. We also saw release of adsorbed ^{59}FeEnt from both Δ*fepB* and Δ*tonB* bacteria. However, exposure of the Δ*fepB* strain to FeEnt at 37 °C made FepA residue G54C accessible (32) to fluoresceination, whereas in Δ*tonB* bacteria, which bind but do not transport, the same residue was inaccessible to chemical modification. Even without FepB, therefore, FepA had activity associated with FeEnt transport, whereas without TonB, it was mechanistically inactive. PUB experiments were decisive to the realization that indeed FepA internalized FeEnt in the Δ*fepB* strain, but in the absence of a binding protein in the periplasm, the ligand escaped through TolC and rebound to FepA. This futile transport/leakage cycle underscored the indispensability of periplasmic binding proteins to metal transport. All TonB-dependent OM uptake systems require periplasmic binding proteins (67), so this conclusion about FeEnt acquisition probably generalizes to other ferric siderophore transporters as well. Finally, the discharge of FeEnt through the TolC channel demonstrates the influence of this pathway on the concentrations of even non-antibiotic, nutrilite solutes in the periplasm.

Acknowledgments—We thank W. A. Kaserer for assistance in the construction of bacterial strains and Paul Cook for comments on the manuscript.

REFERENCES

1. Neilands, J. B. (1981) *Annu. Rev. Biochem.* **50,** 715–731
2. Neilands, J. B. (1995) *J. Biol. Chem.* **270,** 26723–26726
3. Konopka, K., Bindereif, A., and Neilands, J. B. (1982) *Biochemistry* **21,** 6503–6508
4. Tidmarsh, G. F., Klebba, P. E., and Rosenberg, L. T. (1983) *J. Inorg. Biochem.* **18,** 161–168
5. North, M. L., Lang, J. M., Bergerat, J. P., Giron, C., Oberling, F., and Mayer, S. (1984) *Nouv. Rev. Fr. Hematol.* **26,** 317–321
6. Cabrales, P., Tsai, A. G., Intaglietta, M., Callaway, J. K., Beart, P. M., Jarrott, B., North, M. L., Lang, J. M., Bergerat, J. P., Giron, C., Oberling, F., and Mayer, S. (2007) *Antioxid. Redox. Signal.* **9,** 375–384
7. Pollack, J. R., and Neilands, J. B. (1970) *Biochem. Biophys. Res. Commun.* **38,** 989–992
8. Buchanan, S. K., Smith, B. S., Venkatramani, L., Xia, D., Esser, L., Palnitkar, M., Chakraborty, R., van der Helm, D., and Deisenhofer, J. (1999) *Nat. Struct. Biol.* **6,** 56–63
9. Rutz, J. M., Liu, J., Lyons, J. A., Goranson, J., Armstrong, S. K., McIntosh, M. A., Feix, J. B., and Klebba, P. E. (1992) *Science* **258,** 471–475
10. Newton, S. M., Igo, J. D., Scott, D. C., and Klebba, P. E. (1999) *Mol. Microbiol.* **32,** 1153–1165
11. Wang, C. C., and Newton, A. (1971) *J. Biol. Chem.* **246,** 2147–2151
12. Guterman, S. K., and Dann, L. (1973) *J. Bacteriol.* **114,** 1225–1230
13. Kadner, R. J. (1990) *Mol. Microbiol.* **4,** 2027–2033
14. Postle, K. (1993) *J. Bioenerg. Biomembr.* **25,** 591–601
15. Postle, K., and Kadner, R. J. (2003) *Mol. Microbiol.* **49,** 869–882

16. Khursigara, C. M., De Crescenzo, G., Pawelek, P. D., and Coulton, J. W. (2005) *Biochemistry* **44,** 3441–3453
17. Postle, K., and Larsen, R. A. (2007) *Biometals* **20,** 453–465
18. Pierce, J. R., Pickett, C. L., and Earhart, C. F. (1983) *J. Bacteriol.* **155,** 330–336
19. Sprencel, C., Cao, Z., Qi, Z., Scott, D. C., Montague, M. A., Ivanoff, N., Xu, J., Raymond, K. M., Newton, S. M., and Klebba, P. E. (2000) *J. Bacteriol.* **182,** 5359–5364
20. Shea, C. M., and McIntosh, M. A. (1991) *Mol. Microbiol* **5,** 1415–1428
21. Brickman, T. J., and McIntosh, M. A. (1992) *J. Biol. Chem.* **267,** 12350–12355
22. Klebba, P. E. (2003) *Front. Biosci.* **8,** 1422–1436
23. Kaserer, W. A., Jiang, X., Xiao, Q., Scott, D. C., Bauler, M., Copeland, D., Newton, S. M., and Klebba, P. E. (2008) *J. Bacteriol.* **190,** 4001–4016
24. Shultis, D. D., Purdy, M. D., Banchs, C. N., and Wiener, M. C. (2006) *Science* **312,** 1396–1399
25. Pawelek, P. D., Croteau, N., Ng-Thow-Hing, C., Khursigara, C. M., Moiseeva, N., Allaire, M., and Coulton, J. W. (2006) *Science* **312,** 1399–1402
26. Higgs, P. I., Larsen, R. A., and Postle, K. (2002) *Mol. Microbiol.* **44,** 271–281
27. Scott, D. C., Cao, Z., Qi, Z., Bauler, M., Igo, J. D., Newton, S. M., and Klebba, P. E. (2001) *J. Biol. Chem.* **276,** 13025–13033
28. Annamalai, R., Jin, B., Cao, Z., Newton, S. M., and Klebba, P. E. (2004) *J. Bacteriol.* **186,** 3578–3589
29. Miller, J. H. (1972) *Experiments in Molecular Genetics*, p. 433, Cold Spring Harbor Laboratory, Cold Spring Harbor, NY
30. Neidhardt, F. C., Bloch, P. L., and Smith, D. F. (1974) *J. Bacteriol.* **119,** 736–747
31. Klebba, P. E., McIntosh, M. A., and Neilands, J. B. (1982) *J. Bacteriol.* **149,** 880–888
32. Ma, L., Kaserer, W., Annamalai, R., Scott, D. C., Jin, B., Jiang, X., Xiao, Q., Maymani, H., Massis, L. M., Ferreira, L. C., Newton, S. M., and Klebba, P. E. (2007) *J. Biol. Chem.* **282,** 397–406
33. Datsenko, K. A., and Wanner, B. L. (2000) *Proc. Natl. Acad. Sci. U.S.A.* **97,** 6640–6645
34. Wayne, R., and Neilands, J. B. (1975) *J. Bacteriol.* **121,** 497–503
35. Udho, E., Jakes, K. S., Buchanan, S. K., James, K. J., Jiang, X., Klebba, P. E., and Finkelstein, A. (2009) *Proc. Natl. Acad. Sci. U.S.A.* **106,** 21990–21995
36. Cao, Z., Warfel, P., Newton, S. M., and Klebba, P. E. (2003) *J. Biol. Chem.* **278,** 1022–1028
37. Ames, G. F. (1974) *J. Biol. Chem.* **249,** 634–644
38. Murphy, C. K., Kalve, V. I., and Klebba, P. E. (1990) *J. Bacteriol.* **172,** 2736–2746
39. Cao, Z., Qi, Z., Sprencel, C., Newton, S. M., and Klebba, P. E. (2000) *Mol. Microbiol.* **37,** 1306–1317
40. Payne, M. A., Igo, J. D., Cao, Z., Foster, S. B., Newton, S. M., and Klebba, P. E. (1997) *J. Biol. Chem.* **272,** 21950–21955
41. Arrhenius, S. (1889) *Zeitschrift fur Physikalische Chemie* **4,** 226–248
42. Smit, J., Kamio, Y., and Nikaido, H. (1975) *J. Bacteriol.* **124,** 942–958
43. Smallwood, C. R., Marco, A. G., Xiao, Q., Trinh, V., Newton, S. M., and Klebba, P. E. (2009) *Mol. Microbiol.* **72,** 1171–1180
44. Bradbeer, C. (1993) *J. Bacteriol.* **175,** 3146–3150
45. Bleuel, C., Grosse, C., Taudte, N., Scherer, J., Wesenberg, D., Krauss, G. J., Nies, D. H., and Grass, G. (2005) *J. Bacteriol.* **187,** 6701–6707
46. Stephens, D. L., Choe, M. D., and Earhart, C. F. (1995) *Microbiology* **141,** 1647–1654
47. Bowen, H. J. (1966) *Trace Elements in Biochemistry*, Academic Press, Inc., New York
48. Neilands, J. B. (1974) in *Microbial Iron Metabolism: A Comprehensive Treatise* (Neilands, J. B., ed) Vol. 1, pp. 4–34, Academic Press, Inc., New York
49. Wang, C. C., and Newton, A. (1969) *J. Bacteriol.* **98,** 1142–1150
50. Hancock, R. W., and Braun, V. (1976) *J. Bacteriol.* **125,** 409–415
51. Bradbeer, C., and Woodrow, M. L. (1976) *J. Bacteriol.* **128,** 99–104
52. Reynolds, P. R., Mottur, G. P., and Bradbeer, C. (1980) *J. Biol. Chem.* **255,** 4313–4319
53. Nikaido, H., and Vaara, M. (1985) *Microbiol. Rev.* **49,** 1–32
54. Konisky, J. (1979) in *Bacterial Outer Membranes: Biogenesis and Function* (Inouye, M., ed) pp. 319–359, John Wiley and Sons, New York
55. Gudmundsdottir, A., Bell, P. E., Lundrigan, M. D., Bradbeer, C., and Kadner, R. J. (1989) *J. Bacteriol.* **171,** 6526–6533
56. Letain, T. E., and Postle, K. (1997) *Mol. Microbiol.* **24,** 271–283
57. Larsen, R. A., Letain, T. E., and Postle, K. (2003) *Mol. Microbiol.* **49,** 211–218
58. Chang, C., Mooser, A., Plückthun, A., and Wlodawer, A. (2001) *J. Biol. Chem.* **276,** 27535–27540
59. Kojima, S., and Blair, D. F. (2001) *Biochemistry* **40,** 13041–13050
60. Zhai, Y. F., Heijne, W., and Saier, M. H., Jr. (2003) *Biochim. Biophys. Acta* **1614,** 201–210
61. Bradbeer, C., Kenley, J. S., Di Masi, D. R., and Leighton, M. (1978) *J. Biol. Chem.* **253,** 1347–1352
62. Bassford, P. J., Jr., Bradbeer, C., Kadner, R. J., and Schnaitman, C. A. (1976) *J. Bacteriol.* **128,** 242–747
63. Klebba, P. E. (2004) *Iron Transport in Bacteria: Molecular Genetics, Biochemistry, Microbial Pathogenesis and Ecology* (Crosa, J. H., and Payne, S. M., eds) pp. 147–157, American Society for Microbiology Press, Washington, D. C.
64. Gutfreund, H. (1995) *Kinetics for the Life Sciences: Receptors, Transmitters and Catalysts*, pp. 233–234, Cambridge University Press, Cambridge, UK
65. Breidenstein, E., Mahren, S., and Braun, V. (2006) *J. Bacteriol.* **188,** 6440–6442
66. Braun, V., and Endriss, F. (2007) *Biometals* **20,** 219–231
67. Krewulak, K. D., and Vogel, H. J. (2008) *Biochim. Biophys. Acta* **1778,** 1781–1804